10.0
File

NATIONAL BUREAU OF STANDARDS REPORT

8064

A VELOCITY MODULATED TIME-OF-FLIGHT MASS SPECTROMETER

By

R. M. Mills

◇NBS◇

U. S. DEPARTMENT OF COMMERCE
NATIONAL BUREAU OF STANDARDS

THE NATIONAL BUREAU OF STANDARDS

Functions and Activities

The functions of the National Bureau of Standards include the development and maintenance of the national standards of measurement and the provision of means and methods for making measurements consistent with these standards; the determination of physical constants and properties of materials; the development of methods and instruments for testing materials, devices, and structures; advisory services to government agencies on scientific and technical problems; invention and development of devices to serve special needs of the Government; and the development of standard practices, codes, and specifications, including assistance to industry, business and consumers in the development and acceptance of commercial standards and simplified trade practice recommendations. The work includes basic and applied research, development, engineering, instrumentation, testing, evaluation, calibration services, and various consultation and information services. Research projects are also performed for other government agencies when the work relates to and supplements the basic program of the Bureau or when the Bureau's unique competence is required. The scope of activities is suggested by the listing of divisions and sections on the inside of the back cover.

Publications

The results of the Bureau's research are published either in the Bureau's own series of publications or in the journals of professional and scientific societies. The Bureau itself publishes three periodicals available from the Government Printing Office: The Journal of Research, published in four separate sections, presents complete scientific and technical papers; the Technical News Bulletin presents summary and preliminary reports on work in progress; and Central Radio Propagation Laboratory Ionospheric Predictions provides data for determining the best frequencies to use for radio communications throughout the world. There are also seven series of nonperiodical publications: Monographs, Applied Mathematics Series, Handbooks, Miscellaneous Publications, Technical Notes, Commercial Standards, and Simplified Practice Recommendations.

A complete listing of the Bureau's publications can be found in National Bureau of Standards Circular 460, Publications of the National Bureau of Standards, 1901 to June 1947 ($1.25), and the Supplement to National Bureau of Standards Circular 460, July 1947 to June 1957 ($1.50), and Miscellaneous Publication 240, July 1957 to June 1960 (includes Titles of Papers Published in Outside Journals 1950 to 1959) ($2.25); available from the Superintendent of Documents, Government Printing Office, Washington, D.C., 20402.

NATIONAL BUREAU OF STANDARDS REPORT

A VELOCITY MODULATED TIME-OF-FLIGHT MASS SPECTROMETER

By

R. M. Mills

<NBS>

U. S. DEPARTMENT OF COMMERCE

NATIONAL BUREAU OF STANDARDS

A VELOCITY MODULATED TIME-OF-FLIGHT MASS SPECTROMETER*

By

R. M. Mills

ABSTRACT

This paper discusses the possibility of
using velocity modulation to improve a time-
of-flight mass spectrometer. Calculations
show that the resolution can be greatly in-
creased while keeping the unusually high duty
cycle. Previously experienced difficulties
with harmonics are expected to be significantly
reduced by the use of velocity modulation.

The resolution has been calculated for
three experimental arrangements. The sim-
plest yields a resolution of 650 at 80% duty
cycle. If a special "correction wave" gen-
erator is added, a resolution of 13,000 at
86% duty cycle seems possible. The third
arrangement is a variation of the first which
avoids certain grounding difficulties. It
is shown that this gives approximately the
same resolution and duty cycle as does the
first.

Equations are derived giving general
expressions for resolution and duty cycle
for the simplest velocity modulated arrange-
ment. Finally, a rough experimental veri-
fication of the velocity modulated scheme
is given.

1. Introduction

A time-of-flight mass spectrometer has been built which
is capable of operating at an unusually high duty cyle [1].
Ions are first accelerated through a constant d-c voltage
and then pass into a cylindrical drift tube about a meter
long. A radio frequency (rf) sine voltage is applied at
the exit and entrance gaps of the drift tube in such a way
that the field at the entrance is the negative of that at

---

the exit. Ions of mass m which travel through the drift tube in any whole number of rf cycles, n, therefore experience no net change in energy. These ions which experience no energy change are referred to as resonant ions. Mass discrimination is achieved by measuring the number of resonant ions that arrive at the collector located after the drift tube. It is assumed that both gap widths are small so that the transit-time through the rf fields is taken to be zero [1].

Besides high duty cycle, this instrument offers advantages of simplicity and light weight. However, it has two serious limitations. Its resolution is moderately low (about 40), and the presence of harmonics (for a given mass, there are peaks for every whole number value of n) makes the instrument most useful in applications requiring the analysis of a simple mass spectrum.

This scheme assumes that the velocity of the ions passing through the drift tube depends only on the mass of the ions and the d-c voltage through which the ions are accelerated before entering the drift tube. It is shown in [1] that the resolution is limited by the influence which the rf voltage at the entrance gap has on the velocity of the ions as they travel through the drift tube, referred to as velocity modulation. The flight time of the ions through the drift tube depends on the instantaneous value of the rf field at the entrance gap to a significant degree, even though the peak to peak value of the rf voltage is only a few per cent of the d-c accelerating voltage.

This paper suggests a scheme whereby velocity modulation can be used to improve resolution while keeping the high duty cycle, and to reduce the cluttering due to the presence of the harmonics.

2. The Velocity Modulation Scheme

Figure 1 is a simplified schematic diagram of the proposed velocity modulated time-of-flight mass spectrometer. As before, ions accelerate through a d-c voltage, V_{dc}, and then pass through the drift tube entrance gap, (a), across which a radio frequency saw tooth voltage, V_{st}, is applied. The saw tooth voltage applied at both the entrance (a) and exit (c) gaps rises linearly with time until the instantaneous flyback. To the first approximation, ions entering the drift tube at phase ωt can be made to bunch at the midpoint of the drift tube, and

continue their flight to exit through gap (c) at phase -ωt by choosing the proper ratio of V_{st}/V_{dc}. See Figure 2. This means that the last ions of a particular rf cycle to enter gap (a) are the first to exit through gap (c). Referring to Figure 2, it is seen that the ions receive V_{st} (τ/T) electron volts at (a) from the rf wave and $-V_{st}$(τ/T) at (c). Here τ is the time at which the ions traverse the entrance gap and T is the period of the rf voltage. τ is defined only when -T/2 < τ < T/2 and is equal to zero when the r.f. voltage is zero during the rising portion of the saw tooth wave. As before, the resonant ions neither gain nor lose energy from the applied rf fields and the same detection system as described in [1] which measures the number of ions experiencing no net energy change can be used. This measurement is made by the retarding field method [2],[3]. Since the discussion which follows depends on an understanding of the retarding field method, a review from reference [1] will be given.

After leaving the drift tube through gap (c), the ions are decelerated through a potential of $-V_{dc}$. They then approach an electrical barrier placed immediately in front of the Faraday cage collector. For a given barrier potential, E, measured with respect to the ion source, only ions with energies equal to E electron volts or greater can pass. The relationship between S(E), defined as the number of ions per unit of time that penetrate a barrier of height E, and N(e), defined as the number of ions approaching the barrier per unit time with energy between e and e+de at the barrier, can be expressed as:

$$S(E) = \int_{E}^{\infty} N(e) \, de$$

Since the detection system must measure the number of ions which have had their energies unchanged by the rf fields and since these particular ions arrive at the barrier with the same energy that they had at the source, N(e) at the point where e = 0 is the quantity sought. N(e) is obtained from the above equation by differentiating with respect to E:

$$\frac{dS(E)}{dE} = -N(e) \Big\} \text{ at the point where e = E}$$

The differentiation is approximated in the instrument by intro-
ducing a variation in E, ΔE, about the point E = 0. S(E) is
proportional to the collector current. The variation in collec-
tor current, or the a-c component, is therefore approximately
proportional to -N (e) for a given ΔE. Using ΔE of finite
size means that an average value of -N(e) is actually measured
over the range of e = 0 ± ΔE. The variation in ion current is
amplified by a-c amplifiers and fed to synchronous detectors,
ΔE supplying the reference signal used in the detector.

Returning to the discussion of the velocity modulation
scheme, two modifications of the arrangement shown in Figure 1
have been studied. It will be shown that an even greater im-
provement in resolution results if an additional rf wave, called
the correction wave (e_c), is applied to the exit gap (c) as
shown in Figure 3.

The schemes pictured in Figures 1 and 3 have the practical
disadvantage that one, but not both of the end grids, shown as
dotted lines, can be at rf ground potential. Therefore, either
the ion source or collector must follow the rf voltage in order
to insure that the ions receive energy from the rf voltage only
at gaps (a) and (c). To avoid this complication, the scheme
shown in Figure 4 was studied. Two separate, but synchronized,
sawtooth generators are employed, one producing a linearly rising
voltage and the other a linearly falling voltage, the latter
generator being connected with its polarity reversed. The end
grids at gaps (a) and (c) are at rf ground. It can be seen in
Figure 4 that the resulting fields at gaps (a) and (c), going
from left to right, are linearly rising. This is a necessary
condition for operation of a velocity modulated mass spec-
trometer. All resonant ions are bunched when they reach gap (b)
at a time when the rf voltage goes through zero. The wave
form at (b) therefore, does not influence the resonant ions.

3. Calculations

A glossary of symbols is included at the back of this
paper.

3a. RF Wave Shape

The kinetic energy may be equated to the potential energy
through which an ion has fallen and solved for transit time:

$$t_{(ac)} = L_{(ac)} \sqrt{\frac{m}{2qV_{dc}}} \left[\sqrt{\frac{1}{1 + \frac{V_{rf}}{V_{dc}}}} \right] = t_{o(ac)} \sqrt{\frac{1}{1 + \frac{V_{rf}}{V_{dc}}}} \tag{1}$$

where $t_{(ac)}$ is the time taken by ions to travel between (a) and (c), $L_{(ac)}$ is the distance between (a) and (c), m is the mass of the ions, $t_{o(ac)}$ is the flight time of an ion when τ = 0 between (a) and (c), and q is the charge of the ion. As explained in Section 2, the device depends on the rf voltage at $-\omega\tau$ being the negative of that at $+\omega\tau$. The desired rf wave form therefore has odd symmetry, and the desired flight time for resonance is (see figure 2):

$$t_{(ac)} = t_{o(ac)} - 2\tau \qquad -0.5 < \tau/T < 0.5 \qquad (2)$$

Note that ions which enter late in the cycle (large τ) are subjected to a higher accelerating potential and have a shorter transit time, $t_{(ac)}$. Combining equations (1) and (2), and solving for the rf voltage:

$$\frac{V_{rf}}{V_{dc}} = \frac{1}{\left[1 - \dfrac{2\tau}{t_{o(ac)}}\right]^2} - 1 = 4\frac{\tau}{t_{o(ac)}} + 12\left[\frac{\tau}{t_{o(ac)}}\right]^2 + \cdots \qquad (3)$$

In the above equation, τ must be much smaller than $t_{o(ac)}$ so that the second order term (and higher) can be neglected. Otherwise the expression does not have odd symmetry and equation (2) is not valid. This requirement means that higher harmonics must be used. If $\tau << t_{o(ac)}$, equation (3) reduces to an expression showing that V_{rf} should be a linear function of entrance time, τ. It is thus shown that a sawtooth voltage is the proper wave form to produce, to the first approximation, the desired velocity modulation in Figure 1.

3b. Peak Shapes of Scheme in Figure 1

Define e_{rf} as the net energy, in electron volts, which an ion receives from the entrance and exit rf fields. e_{rf} is equal to zero for resonant ions. e_{rf} can be expressed as a function of the difference between two numbers, $n_{1(ac)}$ and $n_{2(ac)}$. $n_{1(ac)}$ is the number of rf cycles taken by any velocity modulated ion to travel through the drift tube and is equal to $t_{(ac)}/T$. $n_{2(ac)}$ is the number of rf cycles taken by velocity modulated resonant ions and is equal to $\dfrac{t'_{o(ac)} - 2\tau}{T}$ where $t'_{o(ac)}/T$ is a whole number.

From the definitions above, it is clear that if $n_{1(ac)} = n_{2(ac)}$, e_{rf} will be equal to zero. However, if the number of rf cycles taken by a velocity modulated ion is different from $n_{2(ac)}$ by some fraction of a cycle, e_{rf} will be equal to the peak rf voltage times that fraction. For example, if an ion

takes 1/4 of a cycle longer than $n_{2(ac)}$ to pass between gaps (a) and (c), e_{rf} will be equal to $V_{st}/4$. Since the rf voltage rises linearly with time, e_{rf} can be expressed as follows over most of the possible values of τ:

$$e_{rf} = V_{st} \left[n_{1(ac)} - n_{2(ac)} \right] \qquad (4)$$

$n_{1(ac)}$ is determined physically by the mass of the ion. It is possible to use a number of values for $n_{2(ac)}$ in equation (4) corresponding to the whole number values of $t'_{o(ac)}/T$. However, it is understood that $n_{2(ac)}$ will be chosen so as to minimize the absolute value of $[n_{1(ac)} - n_{2(ac)}]$. Difficulties may arise if τ is near ± 0.5 or if the absolute value of $[n_{1(ac)} - n_{2(ac)}]$ is large. See appendix.

Substituting for values of $n_{1(ac)}$ and $n_{2(ac)}$ in equation (4), and using equation (1) to express $t_{(ac)}$:

$$\frac{e_{rf}}{V_{st}} = \left[\frac{t_{o(ac)}}{T \sqrt{1 + A \frac{\tau}{T}}} - \frac{t'_{o\ (ac)} - 2\tau}{T} \right]$$

As a special case of $n_{1(ac)}$, define $n_{o(ac)}$ as the number of of rf cycles taken by <u>any</u> ion <u>passing through gap (a) at $\tau = 0$.</u> $n_{o(ac)}$ can also be expressed as $t_{o(ac)}/T$. Likewise, define as a special case of $n_{2(ac)}$ the new variable, $n'_{o(ac)}$, equal to the number of rf cycles taken by a <u>resonant</u> ion which <u>passes through</u> gap (a) at $\tau = 0$. $n'_{o(ac)}$ is equal to $\dfrac{t'_{o(ac)}}{T}$.

The above equation can now be written as:

$$\frac{e_{rf}}{V_{st}} = \left[\frac{n_{o(ac)}}{\sqrt{1 + As}} - n'_{o(ac)} + 2s \right] \qquad (5)$$

where $s = \tau/T$ and $A = \dfrac{V_{st}}{V_{dc}}$. A is to be considered constant. Its proper value for obtaining the desired velocity modulation is calculated as follows. When $\tau = T/2$, $V_{rf} = 1/2 V_{st}$. Therefore,

neglecting higher order terms in equation (3):

$$\frac{V_{st}}{2V_{dc}} = \frac{2T}{t_{o(ac)}}$$

At resonance, $t_{o(ac)} = t'_{o(ac)} = n'_{o(ac)} T$, so:

$$\frac{V_{st}}{V_{dc}} = A = \frac{4}{n'_{o(ac)}} \qquad\qquad (6)$$

It will be useful to plot e_{rf}/V_{st} as a function of s, using the above value of A in equation (5). The task is simplified by first plotting e_{rf}/V_{st} for $n_{o(ac)} = n'_{o(ac)}$ and then finding the other curves by using the approximation:

$$\frac{e_{rf}}{V_{st}}\bigg|_{n_{o(ac)} + \Delta n_{o(ac)}} = \frac{e_{rf}}{V_{st}}\bigg|_{n_{o(ac)}} + \Delta n_{o(ac)} \qquad (7)$$

Equation (7) postulates that the value of e_{rf}/V_{st} at a point a small distance away, $\Delta n_{o(ac)}$, from the original independent variable, $n_{o(ac)}$, is equal to e_{rf}/V_{st} at the original point plus $\Delta n_{o(ac)}$. In other words, equation (7) says that the change in dependent variable is equal to the change in independent variable which is true if:

$$\frac{d(e_{rf}/V_{st})}{d\, n_{o(ac)}} = 1$$

From equation (5) it is seen that:

$$\frac{d(\, e_{rf}/V_{st})}{d\, n_{o(ac)}} = \frac{1}{\sqrt{1 + As}}$$

which is within 2% of unity for the worst case of s (A $\equiv$ 1/10).

Figure 5 is a set of e_{rf}/V_{st} curves for $n'_{o(ac)}$ equal to 37 through 41. A was taken as $4/n'_{o(ac)}$ = 1/10. The non-zero values of e_{rf}/V_{st} for the $n'_{o(ac)}$ = 40 curve when s $\neq$ 0 are the result of neglecting higher order terms in equation (3).

The duty cycle can be found from Figure 5 by noting what fraction of a cycle e_{rf}/V_{st} stays within arbitrarily chosen limits. In figure 6, the peak shapes are plotted for $0.00 < e_{rf}/V_{st} < 0.026$. It is seen that the peak heights decrease as $n'_{o(ac)}$ is changed from a value of $4/A$. Define $n'_{o(ac)}$ as that particular value of n'_{o} which is equal to $4/A$ and produces the highest duty cycle peak.

The presence of multiple harmonics (discussed in Reference 1) is reduced, but not eliminated. Here, though, there is much more space between successive harmonic peaks, thus reducing the problem of cluttering in a complex mass spectrum. For the case shown, the resolution appears to be about 650 with a duty cycle of 80%.

3c.   Peak Shapes of Scheme in Figure 3:

The ideal curve shape for e_{rf}/V_{st} versus s is a horizontal line for the $n''_{o(ac)}$ harmonic and vertical lines corresponding to all other values of $n_{o(ac)}$. One way to approach this condition is to apply an additional rf voltage, called the correction wave (e_c), to the final gap, (c). This correctional wave should be equal to the negative of the e_{rf}/V_{st} versus exit time curve. The transformation of Figure 5 from entrance to exit time does not change the curve shape to any great degree. It thus seems possible that the proper e_c wave shape can be approximated by a full wave rectification of a sine wave which has a period double that of V_{rf}, or $2T$. Calculations were done to find what the curves in Figure 5 would look like if an e_c of this form is added to the last gap. Rather than transforming all of the curves in Figure (5) to exit time, it was easier to change e_c to entrance time. A new set of curves corresponding to Figure 5 was drawn (see Figure 7) and from these, the peak shapes were found as before. The expression corresponding to equation (5) is:

$$\frac{e_{rf}}{V_{st}} = \frac{n_{o(ac)}}{\sqrt{1 + As}} = n'_{o(ac)} + 2s - C\,(1 - \cos \pi s)$$

where C is the amplitude of e_c. Therefore, the approximation given in equation (7) still holds to the same degree of validity. Figure 8 shows the peaks for values of $n'_{o(ac)}$ from 38 to 41 with the arbitrary limit of the differentiating voltage chosen to be $-0.005 < \dfrac{e_{rf} + e_c}{V_{st}} < 0$. The resolution in this case appears to be about 13,000 with a duty cycle of 86%.

3d. Peak Shapes of Scheme in Figure 4

It will be shown that the final e_{rf} for this case is, to a good approximation, the same as the case shown in Figure 1. In order to simplify nomenclature, define e_{rf}/V_{st} for the Figure 1 scheme as F. Also let the subscripts (a) and (c) denote a quantity at or between the appropriate gaps. For example, $t_{(ac)}$ is the flight time between (a) and (c), and $e_{rf(b)}$ is the rf energy in electron volts received at (b), the center gap.

As was mentioned earlier, the resonant ions are bunched at the center gap. If the frequency of the rf voltage is such that $n_{o(ac)}$ is an even, whole number, the bunch of resonant ions will traverse gap (b) when the rf voltage is zero and $e_{rf(b)}$ is zero. If the number, $n_{1(ab)}$, of rf cycles taken by an ion to travel between (a) and (b) is different from the number $n_{2(ab)}$, taken by a resonant ion to travel the same distance, $e_{rf(b)}$ is not zero. Note that the rf voltage at (b) is twice that at (a) and (c), and has the opposite sign. It can be seen that:

$$e_{rf(b)} = -2V_{st}(n_{1(ab)} - n_{2(ab)})$$

The net energy received at (a) and (c) is as before:

$$e_{rf(ac)} = V_{st}(n_{1(ac)} - n_{2(ac)})$$

The total energy received from the rf fields by an ion passing through the three gaps is:

$$e_{rf(\Sigma)} = -2V_{st}(n_{1(ab)} - n_{2(ab)}) + V_{st}(n_{1(ac)} - n_{2(ac)})$$

In the above equation $n_{1(ab)}$, $n_{1(ac)}$, $n_{2(ac)}$, and $n_{2(ab)}$ can be expanded as follows:

$$n_{1(ab)} = \frac{t_{(ab)}}{T} = \frac{L_{(ab)}}{T} \sqrt{\frac{m}{2qV_{dc}}} \left[\sqrt{\frac{1}{1 + \frac{V_{st}}{V_{dc}}\frac{\tau}{T}}} \right]$$

Or:

$$n_{1(ab)} = n_{o(ab)} \sqrt{\frac{1}{1 + As}}$$

$$n_{1(ac)} = \frac{t_{(ac)}}{T} = \frac{L_{(ab)}}{T}\sqrt{\frac{m}{2qV_{dc}}} \left[\sqrt{\frac{1}{1 + \frac{V_{st}}{V_{dc}}\frac{\tau}{T}}} \right] + \frac{L_{(bc)}}{T}\sqrt{\frac{m}{2qV_{dc}}} \left[\sqrt{\frac{1}{1 + \frac{V_{st}}{V_{dc}}\frac{\tau}{T} + \frac{e_{rf(b)}}{V_{dc}}}} \right]$$

Or:

$$n_{1(ac)} = n_{o(ab)} \sqrt{\frac{1}{1 + As}} + n_{o(bc)} \sqrt{\frac{1}{1 + As + \frac{Ae_{rf(b)}}{V_{st}}}}$$

$$n_{2(ac)} = \frac{t_{o(ac)} - 2\tau}{T}$$

$$n_{2(ab)} = \frac{t_{o(ab)} - \tau}{T}$$

Since $t_{o(ac)} = 2t_{o(ab)}$ (if this isn't true, different V_{dc} can be applied to the first and second drift tubes so that $t_{o(ac)}$ is twice $t_{o(ab)}$):

$$n_{2(ac)} = 2n_{2(ab)} = 2n_{2(bc)}$$

$n_{1(ac)}$ can now be expressed as:

$$n_{1(ac)} = n_{o(ab)} \sqrt{\frac{1}{1 + As}} + n_{o(ab)} \sqrt{\frac{1}{1 + As + \frac{Ae_{rf(b)}}{V_{st}}}}$$

Making use of the above equation, $e_{rf(\Sigma)}$ can be written as:

$$\frac{e_{rf(\Sigma)}}{V_{st}} = -\left[\frac{2n_{o(ab)}}{\sqrt{1 + As}} - 2n_{2(ab)}\right] + \left[\frac{n_{o(ab)}}{\sqrt{1 + As}} + \frac{n_{o(ab)}}{\sqrt{1 + As + \dfrac{Ae_{rf(b)}}{V_{dc}}}} - 2n_{2(a}\right.$$

or:

$$\frac{e_{rf(\Sigma)}}{V_{st}} = n_{o(ab)}\left[\frac{1}{\sqrt{1 + As + \dfrac{Ae_{rf(b)}}{V_{st}}}} - \frac{1}{\sqrt{1 + As}}\right] \qquad (8)$$

Expanding equation (8) using the first two terms of the binomial expansion:

$$\frac{e_{rf(\Sigma)}}{V_{st}} \cong n_{o(ab)}\left[1 - \frac{As}{2} - \frac{A}{2}\frac{e_{rf(b)}}{V_{st}} - 1 + \frac{As}{2}\right]$$

$$\frac{e_{rf(\Sigma)}}{V_{st}} \cong -\frac{n_{o(ab)}}{2}\frac{Ae_{rf(b)}}{V_{st}}$$

But:

$$e_{rf(b)} = -2V_{st}\left[n_{1(ab)} - n_{2(ab)}\right]$$

$$e_{rf(b)} = -V_{st}\left[2n_{1(ab)} - 2n_{2(ab)}\right] = -V_{st}F$$

And $A = 4/n''_{o(ac)} = 2/n''_{o(ab)}$

Therefore:

$$\frac{e_{rf(\Sigma)}}{V_{st}} \cong \frac{n_{o(ab)}}{n''_{o(ab)}}F = \frac{n_{o(ac)}}{n''_{o(ac)}}F \qquad (9)$$

The net rf energy which the ions receive is therefore the same as with the scheme shown in figure 1 when $n_{o(ac)}$ is near $n''_{o(ac)}$, with one important exception. If $n_{o(ac)}$ = $n'_{o(ac)}$ is an odd number, $n_{o(ab)}$ will not be a whole number. This means that the resonant ion bunch goes through (b) at a time when the rf voltage is at a maximum giving the ion between $\pm V_{st}$ electron volts. The exact result is hard to predict because of the discontinuity in the rf voltage at $\omega\tau = \pi$, but it should be safe to assume that the odd harmonics (i.e. odd values of $n'_{o(ac)}$ will be greatly reduced, if not eliminated. The absence of the odd harmonics reduces further the cluttering problem mentioned in [1].

When $n_{o(ac)}$ is not equal to $n''_{o(ac)}$, $e_{rf(\Sigma)}$ is changed by a factor of $n_{o(ac)}/n''_{o(ac)}$. The effect on the peak shapes is a more rapid disappearance of harmonics as $n_{o(ac)}$ is increased above $n''_{o(ac)}$ and a more gradual disappearance of the harmonics for $n_{o(ac)}$ less than $n''_{o(ac)}$.

The actual resolution of the $n''_{o(ac)}$ harmonic for the scheme shown in Figure 4 was calculated without using the binomial expansion approximation [i.e. by using equation (8)]. The results, resolution of 660 at 75% maximum duty cycle, are nearly the same as those given in section B (resolution of 650 at 80% maximum duty cycle), thereby reaffirming the conclusion that the binomial expansion approximation results in the same expressions for e_{rf} as the scheme shown in figure 1.

3e. Maximum Duty Cycle

One of the principal attributes of the mass spectrometer described in [1] is its high duty cycle. It has been shown that velocity modulation can be used to achieve a considerable increase in resolution. An approximate expression for maximum duty cycle for the velocity modulated instrument can be derived to show that the increase in resolution has not been made at the expense of the duty cycle.

The derivation is based on equation (5), which was derived for the Figure 1 scheme. If conditions are such that the absolute value of both $\left(As + A\dfrac{e_{rf(b)}}{V_{st}}\right)$ and As are small compared to unity so equation (8) can be represented accurately by the first two terms of the binomial expansion, the following derivation applies to the schemes of both Figures 1 and 4 since the maximum duty cycle occurs when $n_{o(ac)} = n'_{o(ac)} = n''_{o(ac)}$.

Equation (5) can be expanded as follows:

$$\frac{e_{rf}}{V_{st}} = n_{o(ac)}\left[1 - \frac{As}{2} + 3/8\,A^2s^2 - 5/16\,A^3s^3 + \ldots\right] - n'_{o(ac)} + 2s \tag{10}$$

Since A is equal to $4/n''_{o(ac)}$:

$$\frac{e_{rf}}{V_{st}} \cong \left[n_{o(ac)} - n'_{o(ac)}\right] + 2\left[1 - \frac{n_{o(ac)}}{n''_{o(ac)}}\right]s + 6\frac{n_{o(ac)}s^2}{n''_{o(ac)^2}} - 20\frac{n_{o(ac)}s^3}{n''_{o(ac)^3}} \tag{11}$$

The maximum duty cycle occurs when $n_{o(ac)} = n'_{o(ac)} = n''_{o(ac)}$. Making this substitution and neglecting the last term, equation (11) becomes:

$$\frac{e_{rf}}{V_{st}} \cong \frac{6s^2}{n''_{o(ac)}} \tag{12}$$

The minimum of the e_{rf}/V_{st} curve for the $n''_{o(ac)}$ harmonic is at the origin (See Fig. 5). The differentiating voltage used for detection should therefore swing between zero and some arbitrarily chosen upper limit, say α. The maximum duty cycle is found by solving equation (12) for s with e_{rf}/V_{st} equal to α and multiplying by two in order to account for the positive and negative values of s. This quantity is the fraction of the rf cycle for which e_{rf}/V_{st} is between 0 and α and thus is the desired expression:

$$\text{Maximum Duty Cycle} = 2\sqrt{\frac{\alpha\,n''_{o(ac)}}{6}} \tag{13}$$

3f.   Approximate Resolution of the n_o'' Harmonic

An approximate expression for the resolution when $n_{o(ac)} = n_{o(ac)}''$ can also be derived from equation (12). As before, the derivation applies to the scheme in Figure 1 and under some conditions to the Figure 4 scheme as well. By definition introduced earlier:

$$t_{o(ac)} = n_{o(ac)} \; T = L_{(ac)} \sqrt{\frac{m}{2qV_{dc}}}$$

Therefore for a small change in m, $\triangle$ m:

$$\frac{m}{\triangle m} = 1/2 \; \frac{n_{o(ac)}}{\triangle n_{o(ac)}} \tag{14}$$

The estimates of resolution which have been given are based on equation (14), $\triangle n_{o(ac)}$ being measured graphically from curves similar to Figures 5 and 7.

Define $\triangle_+$ and $\triangle_-$ such that their sum is the peak width at half peak height point in figure 9. In order to measure the duty cycle at $n_{o(ac)} = n_{o(ac)}'' + \triangle_+$, the curve corresponding to $n_{o(ac)}'' + \triangle_+$ can be drawn in above the curve corresponding to $n_{o(ac)}''$ in Figure 5, and the points at which this new curve leaves the differentiating region can be determined as before. If equation (7) can be assumed to be valid, the new curve corresponding to $n_{o(ac)}'' + \triangle_+$ is parallel to the $n_{o(ac)}''$ curve and shifted above the $n_{o(ac)}''$ curve by an amount $\triangle_+$. Therefore, instead of drawing a new curve <u>above</u> the one corresponding to $n_{o(ac)}''$, the $n_{o(ac)}''$ curve can be used if it is imagined that the differentiating curve is shifted <u>down</u> by an amount $\triangle_+$. The differentiation zone actually has lower and upper limits of $e_{rf}/V_{st} = 0$ and $e_{rf}/V_{st} = \alpha$. But if it undergoes an imaginary shift down to new limits of $e_{rf}/V_{st} = -\triangle_+$ and $e_{rf}/V_{st} = \alpha - \triangle_+$, the $n_{o(ac)}''$ curve emerges from the zone only at the upper boundry.

To find the value of s where the curve emerges from the differentiation zone, consider equation (11). In this case, the simplification of equation (12) cannot be made without justification since $n_{o(ac)} \neq n''_{o(ac)}$. However, the needed justification can be had from equations (7) and (12). Equation (12) shows that, to a good approximation, e_{rf}/V_{st} varies as the second power of s for the resonance curve. And in equation (7) it is seen that, again to a good approximation, the e_{rf}/V_{st} curve which is different from the resonance curve by $\Delta n_{o(ac)}$ is equal to the resonance curve plus the constant $\Delta n_{o(ac)}$. If this approximation is to be compatible with equation (11), the first and third terms on the right side of equation (11) must be the significant terms, since the first term in equation (11) is the same as the constant in (7). Shifting the differentiation zone is a way of accouting for the constant term in equation (11). Therefore, equation (12) can be used when $n_{o(ac)} = n''_{o(ac)} + \Delta_+$ if it is changed to read:

$$\frac{e_{rf}}{V_{st}} = 6 \frac{n_{o(ac)}}{n''_{o(ac)}^2} s^2 \qquad (12a)$$

Solve equation (12a) for s at the boundry of the shifted differentiation zone where $e_{rf}/V_{st} = \propto - \Delta_+$:

$$s \cong \sqrt{\frac{(\propto - \Delta_+) \, n''_{o(ac)}^2}{6 \, n_{o(ac)}}} \qquad (12b)$$

If equation (12b) is multiplied by 2 to account for the positive and negative values of s, the duty cycle is obtained as before:

$$\text{Duty Cycle At} \quad (n''_o + \Delta_+) = 2\sqrt{\frac{(\propto - \Delta_+) \, n''_{o(ac)}^2}{6 \, n_{o(ac)}}} \qquad (12\ c)$$

The duty cycle at $n_{o(ac)} = n''_{o(ac)} + \Delta_+$ is also known by definition to be 1/2 the maximum expressed in equation (13):

$$\text{1/2 Maximum Duty Cycle} = \sqrt{\frac{\propto \, n''_{o(ac)}}{6}} \qquad (13a)$$

Equating (13a) and (12c):

$$\sqrt{\frac{\alpha\, n''_{o(ac)}}{6}} \cong 2\sqrt{\frac{(\alpha - \Delta_+)n''^{2}_{o(ac)}}{6\, n_{o(ac)}}} = 2\sqrt{\frac{(\alpha - \Delta_+)n''^{2}_{o(ac)}}{6(n''_{o(ac)} + \Delta_+)}}$$

and solving for Δ_+ :

$$\Delta_+ \cong \frac{3 n''_{o(ac)}\, \alpha}{4\, n''_{o(ac)} + \alpha}$$

If $4\, n''_{o(ac)} \gg \alpha$:

$$\Delta_+ \cong 3/4\, \alpha \qquad\qquad (15)$$

In the same way Δ_- can be found by making an imaginary shift of the differentiation zone up by Δ_-. The $n_{o(ac)} = n''_{o(ac)}$ curve now usually leaves the zone at both the upper (i.e. $e_{rf}/V_{st} = \alpha + \Delta_-$) and lower ($e_{rf}/V_{st} = \Delta_-$) limits.

Thus the portion of the s scale which contributes to the output signal will be twice the difference between two terms, one corresponding to upper limit and the other to the lower limit. Again using equation (13) multiplied by 1/2:

$$\sqrt{\frac{\alpha\, n''_{o(ac)}}{6}} \cong 2\left[\sqrt{\frac{(\alpha + \Delta_-)\, n''^{2}_{o(ac)}}{6\, n_{o(ac)}}} - \sqrt{\frac{\Delta_-\, n''^{2}_{o(ac)}}{6\, n_{o(ac)}}}\right]$$

Solving for Δ_- :

$$\Delta_- = \frac{\alpha}{\dfrac{n''_{o(ac)} - \Delta_-}{n''_{o(ac)}}}\left[\frac{1}{16}\left(\frac{n''_{o(ac)} - \Delta_-}{n''_{o(ac)}}\right)^{2} + 1 - 1/2\left(\frac{n''_{o(ac)} - \Delta_-}{n''_o}\right)\right]$$

If $\dfrac{n''_{o(ac)} - \Delta_-}{n''_{o(ac)}}$ is approximately equal to unity:

$$\Delta_- \cong \frac{9}{16}\, \alpha \qquad\qquad (16)$$

It is possible that the $n''_{o(ac)}$ curve leaves the differentiation zone only at the lower limit after the imaginary shift up. If

$$(\alpha + \Delta_-) \; \frac{n''_{o(ac)}}{n''_{o(ac)}{}^{-\Delta_-}} \; > \; 3/2$$

this condition exists. In this case, the derivation of Δ_- , starts with:

$$\sqrt{\frac{\alpha \; n''_{o(ac)}}{6}} \; \cong \; 2 \left[0.5 - \sqrt{\frac{\Delta_- \; n''_{o(ac)}}{6 \; n_{o(ac)}}} \right]$$

However, in practice, α and Δ_- will almost always be small enough so that equation (16) can be used. It will be assumed that this is the case.

Since $\Delta \, n_{o(ac)} = \Delta_- + \Delta_+ = \frac{21}{16} \alpha$, equation (14) can be written as:

$$\frac{m}{\Delta m} \; = \; \frac{8}{21} \; \frac{n''_{o(ac)}}{\alpha}$$

4. Practical Considerations

Three assumptions are made in the above derivations. First, it is assumed that the initial ion energy spread can be neglected. In practice, the energy spread can be made insignificant by using a large V_{dc}. It is shown in [4] that the limit in resolution is:

$$\frac{m}{\Delta m} \; = \; \frac{V}{2V_o}$$

where V is the total energy of an ion in the drift tube and V_o is its initial energy. Thus, V_o determines the lowest value of V_{dc} which can be used to obtain the desired resolution. Second, it is assumed that a satisfactory saw tooth wave generator can be built. That is, the wave must have the necessary linearity at the required frequency and amplitude. The fly back time does not need to be instantaneous since Figure 5 shows that ions which pass gap (a) near $\tau = \pm 0.5T$

are not within the differentiating region anyway. And third, the electrical barrier is assumed to have the necessary energy resolution. Rough estimates of these three assumptions indicate that their validity is good enough for the instrument to operate, but perhaps at a lower duty cycle and resolution than calculated.

Possible parameter values are as follows:

V_{dc} -   3000 volts

V_{st} -   300 volts

$L_{(ac)}$ -   1 meter

Saw Tooth Frequency -   1 to 10 mc

Corresponding Mass Range -   mass 8 to 730

Since the dimensions of the instrument are a few per cent of the fundamental Fouier component wave length at 10 mc, dispersion of the wave shape may become a problem, requiring short transmission lines. In addition to wave dispersion, there will be a phase difference between the waves at gaps (a) and (c). However, this is not expected to cause trouble. Consider Figure 4. If there is a high frequency sine wave on the synchronizing line, there will be a phase difference between the two ends of the line. Express this difference as t_ϕ seconds. Equation (2) should now be changed to

$$t_{(ac)} = t_{o(ac)} + t_\phi - 2\tau \qquad (2a)$$

Combining (2a) and (1) as before and solving for V_{rf}/V_{dc}:

$$\frac{V_{rf}}{V_{dc}} = \frac{1}{\left[1 + \dfrac{t_\phi}{t_o} - \dfrac{2\tau}{t_o}\right]^2} - 1$$

If $\dfrac{t_\phi - 2\tau}{t_o}$ is small compared to unity, the expression for

V_{rf}/V_{dc} can be approximated by a binomial series, neglecting

all terms of the second or higher powers:

$$\frac{V_{rf}}{V_{dc}} \cong \frac{4}{n''_{o(ac)}} \left[\frac{\tau}{T} - 1/2 \frac{t_\phi}{T} \right] = A \left[\frac{\tau}{T} - 1/2 \frac{t_\phi}{T} \right]$$

Or:

$$V_{rf} \cong V_{st} \left[\frac{\tau}{T} - 1/2 \frac{t_\phi}{T} \right]$$

This plots as a linearily increasing voltage with increasing τ. The line is shifted down below the origin by an amount $\frac{V_{st} \, t_\phi}{2T}$. Since the total voltage at the drift tube is

$V_{dc} + V_{rf}$, the same effect can be achieved by leaving V_{rf}

symmetrical about the origin as before, and reducing V_{dc} to $V_{dc} \left[1 - \frac{A \, t_\phi}{2T} \right]$. Normally this will be an insignificant

change. The phase difference between the gaps will also manifest itself by increasing $n''_{o(ac)}$ from a whole number by an amount $\frac{t_\phi}{T}$.

A rough verification of the velocity modulation ideas has been made with the instrument described in [1]. By expanding a sine wave in a power series, it is seen that sin x is a linear wave for small values of x. And since sin (x + π) = - sin x, sin x is also a linear wave having a negative slope when x is near π. The apparatus has the property that the rf voltage applied at gap (a) is the negative of that at gap (c). Thus resonance can occur using the velocity modulation scheme with a sine wave if $n''_{o(ac)}$ is a

whole number plus 1/2. The proper peak to peak sine voltage, still denoted as V_{st}, can be derived by first expanding equation (1) in a binomial series:

$$t_{(ac)} = t_{o(ac)} \left[1 - \frac{V_{rf}}{2V_{dc}} + \ldots \right]$$

If V_{rf}/V_{dc} is small:

$$t_{(ac)} = t_{o(ac)} \left[1 - \frac{V_{st}}{4V_{dc}} \sin \omega\tau \ _{(a)} \right] \qquad (18)$$

where $\tau_{(a)}$ is the time at which an ion passes through gap (a). Unlike τ, $\tau_{(a)}$ has values from 0 to ∞. Let $\tau_{(c)}$ denote the time at which the ion passes gap (c). Then

$$\tau_{(c)} = \tau_{(a)} + t_{(ac)}$$

Using equation (18):

$$\tau_{(c)} = \tau_{(a)} + t_{o(ac)} - \frac{A}{4} t_{o(ac)} \sin \omega\tau_{(a)} \qquad (19)$$

It is shown in simple klystron theory [5] that bunching occurs when

$$\frac{d\,\tau_{(c)}}{d\,\tau_{(a)}} = 0.$$

This means that there is no change in ion arrival time per change in starting time. In the scheme being discussed here, it is required that:

$$\frac{d\,\tau_{(c)}}{d\,\tau_{(a)}} = -1 \qquad (20)$$

In other words, the change in arrival time must be equal to the negative of the change in starting time. An ion starting late by a certain amount must arrive early by the same amount. Differentiating equation (19):

$$\frac{d\,\tau_{(c)}}{d\,\tau_{(a)}} = 1 - \frac{A}{4} t_{o(ac)} \omega \cos \omega\tau_{(a)}$$

$$\frac{d\,\tau_{(c)}}{d\,\tau_{(a)}} = 1 - \frac{A\pi n_{o(ac)}}{2} \cos \omega\tau_{(a)} \qquad (21)$$

Equation (21) equals -1 if $\tau_{(a)}$ is zero and when

$$\frac{A\pi\,n_{o(ac)}}{2} = 2$$

Or:

$$A = \frac{4}{\pi\,n_{o(ac)}}$$

Thus: $V_{st} = \dfrac{V_{dc} \cdot 4}{\pi \; n_{o(ac)}} = \dfrac{12,000}{\pi \; n_{o(ac)}}$ if $V_{dc} = 3,000$ volts.

Or: $V_{st} \cong \dfrac{3820}{n_{o(ac)}}$ volts, peak to peak.

Figure 10 shows some velocity modulated peaks obtained from the reference [1] instrument using a sine rf voltage, for Argon. The velocity modulated peaks are the negative peaks which begin to appear at about $n_{o(ac)} = 23.5$ and increase in intensity until the 26.5 or 27.5 harmonic. The peak to peak sine voltage was set at roughly 145 volts using an oscilloscope. However, the amplitude can not be maintained exactly at this value as the frequency is swept with the present equipment.

The negative direction of the velocity modulated peaks indicate a 180° change between the reference, differentiating voltage and the signal from the Faraday cage. The differentiating voltage is actually applied to the source and the barrier which is in front of the Faraday cage is at a constant potential. As the ions leave the source, they are energy modulated in phase with the reference voltage. When they reach gap (a), they are velocity modulated so that "the first ions to leave (a) are the last to arrive at (c)." The velocity modulation is then neutralized at gap (c). The velocity modulation at gap (a) therefore accounts for the phase shift of the resonant ions between the Faraday signal and reference signal.

No further study has been made of velocity modulation using sine voltages since it is felt that an instrument using a saw tooth wave will be greatly superior, especially in duty cycle. However, Figure 10 and the theoretical discussions on the use of velocity modulation in a time-of-flight mass spectrometer demonstrates the feasibility of building an instrument which has high resolution and high duty cycle.

4. References

[1]   R.M. Mills, "Journal of Research", National Bureau
       of Standards, Section C, Volume 67C, Number 4, Oct.-Dec.

[2]   R.E. Fox, W.M. Hickam, D.J.Grove and T.Kjeldass,Jr.
       "Rev. Sci. Instr." 26, 1101, (1955).

[3]   L.B. Leder and J.A. Simpson, "Rev. Sci. Instr." 29,
       571, (1958).

[4]   H.S. Katzenstein and S.S. Friedland, "Rev. Sci.
       Instr.", 26, 324, (1955).

[5]   "Klystrons and Microwave Triodes", by Donald R.
       Hamilton, Julian K. Knipp, and J.B. Horner Kuper,
       M.I.T. Radiation Laboratory Series No. 7, McGraw-
       Hill Book Co. Inc., New York, (1948), p.206.

5. Glossary of Symbols

$A-$ V_{st}/V_{dc}

$C-$ Amplitude of the correction wave, e_c

e_c- Instantaneous correction wave value

$e_{rf}-$ Net energy, in electron volts, an ion receives from the rf fields.

$e_{rf\overline{\Sigma}}-$ Net energy, in electron volts, an ion receives from the three gaps in the scheme shown in Figure 4

$F-$ e_{rf}/V_{st} for the case shown in Figure 1

$L_{(ac)}-$ Distance between gaps (a) and (c)

$m-$ Mass of ion

$n_{o(ac)}-$ Number of rf cycles taken by an unmodulated ion to travel between gaps (a) and (c). Equal to $t_{o(ac)}/T$

$n'_{o(ac)}-$ Number of rf cycles taken by an unmodulated resonant ion to travel between gaps (a) and (c). Prime denotes a whole number of cyles.

$n''_{o(ac)}-$ That particular value of $n'_{o(ac)}$ equal to $4/A$. A should be adjusted so that $n''_{o(ac)}$ is a whole number.

$n_{1(ac)}-$ Number of rf cycles taken by any velocity modulated ion to travel between gaps (a) and (c). Equal to $t_{(ac)}/T$.

$n_{2(ac)}-$ Number of rf cycles taken by velocity modulated, resonant ions. Equal to $\dfrac{t_{o(ac)} - 2\tau}{T}$

$q-$ Charge of the ion

$s-$ τ/T

$T-$ Period of applied rf voltage

$t_{(ac)}-$ Travel time of an ion between (a) and (c).

$t_{o(ac)}-$ Unmodulated flight time between gaps (a) and (c).

$t'_{o(ac)}-$ Unmodulated flight time of a resonant ion between gaps (a) and (c). Equal to $n'_{o(ac)}t$.

$V_{dc}-$ d-c voltage through which ions are accelerated.

$V_{rf}-$ Instantaneous value of the rf voltage.

$V_{st}-$ Peak to peak value of the rf voltage.

$\Delta_+ -$ $n_{o(ac)} - n'_{o(ac)}$ when the duty cycle is half its maximum value, on the high $n_{o(ac)}$ side of the peak.

$\Delta_- -$ $n_{o(ac)} - n'_{o(ac)}$ when the duty cycle is half its maximum value on the low $n_{o(ac)}$ side of the peak.

$\tau-$ Time at which an ion passes the entrance gap, (a); considered to be the independent time variable.

$\omega-$ Angular frequency of the applied rf voltage.

$\alpha-$ Arbitrarily chosen upper limit of the differentiating voltage in units of e_{rf}/V_{st}.

APPENDIX

The Validity of Equation (4)

Strictly speaking, equation (4) is not valid for all ions because of the discontinuity in the rf voltage. Consider Figure 11, where one cycle during which ions pass through the entrance gap and one cycle during which they leave the drift tube through the exit gap are divided into three periods. The widths of both periods I and II are $(n_{1(ac)} - n_{2(ac)})T$. The expression for e_{rf} in equation (4) is derived by comparing the flight time of the ion in question with a resonant ion. If a resonant ion passes the entrance gap during period I, it will exit during period III. If a non-resonant ion enters during period I, and if it is lighter than the resonant ion such that $n_{1(ac)} - n_{2(ac)} < 0$, the ion exits during period II and equation (4) is valid. The trouble comes when a non-resonant ion leaving during I, is heavier than the resonant ion so that $n_{1(ac)} - n_{2(ac)} > 0$. In this case, the non-resonant ion emerges after the beginning of the next cycle (i.e. after the r.f. voltage fly back). This ion has passed through negative rf fields at both the entrance and exit gaps and therefore experiences a large deceleration instead of the moderate acceleration it would have received if it had started during II or III. In the same way, a non-resonant ion which is lighter than the resonant ion starting during period III experience accelerations at both the entrance and exit gaps, again making e_{rf} larger than predicted in equation (4). In summary, equation (4) is valid when

$$- 0.5 + (n_{1(ac)} - n_{2(ac)}) < \tau/T < 0.5$$

if $n_{1(ac)} - n_{2(ac)}$ is positive and when

$$- 0.5 < \tau/T < 0.5 + (n_{1(ac)} - n_{2(ac)})$$

if $n_{1(ac)} - n_{2(ac)}$ is negative. This means that equation (4) is valid when ions heavier than resonant ions leave during periods II and III and when lighter than resonant ions leave during periods I and II. In all other cases the absolute value of e_{rf} is much larger than that given by equation (4). When the above conditions do not hold equation (4) can be made valid again by changing $n_{2(ac)}$ to $n_{2(ac)} + 1$ when $n_{1(ac)} - n_{2(ac)}$ is positive or to $n_{2(ac)} - 1$ when $n_{1(ac)} - n_{2(ac)}$ is negative.

The above complications are ignored in the derivations that follow. This simplification can be justified by examining the consequences (1) at resonance, (2) near resonance, and (3) far from resonance. (1) At resonance, $n_{1(ac)} - n_{2(ac)} = 0$, so that the exceptions do not apply. (2) Near resonance the effect of using $n_{2(ac)}$ instead of the correct value of $n_{2(ac)} + 1$ or $n_{2(ac)} - 1$ is to make e_{rf} larger than predicted, so that ions which are close enough to resonant ions to be normally represented in the detection system's output signal are excluded from the signal during a fraction of each cycle equal to $n_{1(ac)} - n_{2(ac)}$. In other words, the actual duty cycle is reduced by a factor of $n_{1(ac)} - n_{2(ac)}$ from the calculated value. Note that this effect does not change the peak height at its maximum and causes a more rapid decline as $n_{o(ac)}$ is changed from resonance. Thus, the net effect is a sharpening of the peak shapes. However, this effect is small for case 2 (near resonance) since $n_{1(ac)} - n_{2(ac)}$ is nearly equal to zero.

(3) Far from resonance the use of $n_{2(ac)}$ instead of $n_{2(ac)} + 1$ or $n_{2(ac)} - 1$ results again in a larger absolute value of e_{rf} than calculated, although the increase is not as large as in (2). If the increase in e_{rf} is large enough the ions are not represented in the output signal. In this case the reduction in duty cycle will be larger since $n_{1(ac)} - n_{2(ac)}$ is larger. However, far from resonance the calculated duty cycle is near zero (see Figure 6) and a further reduction is not significant.

FIG. 1

FIG. 2
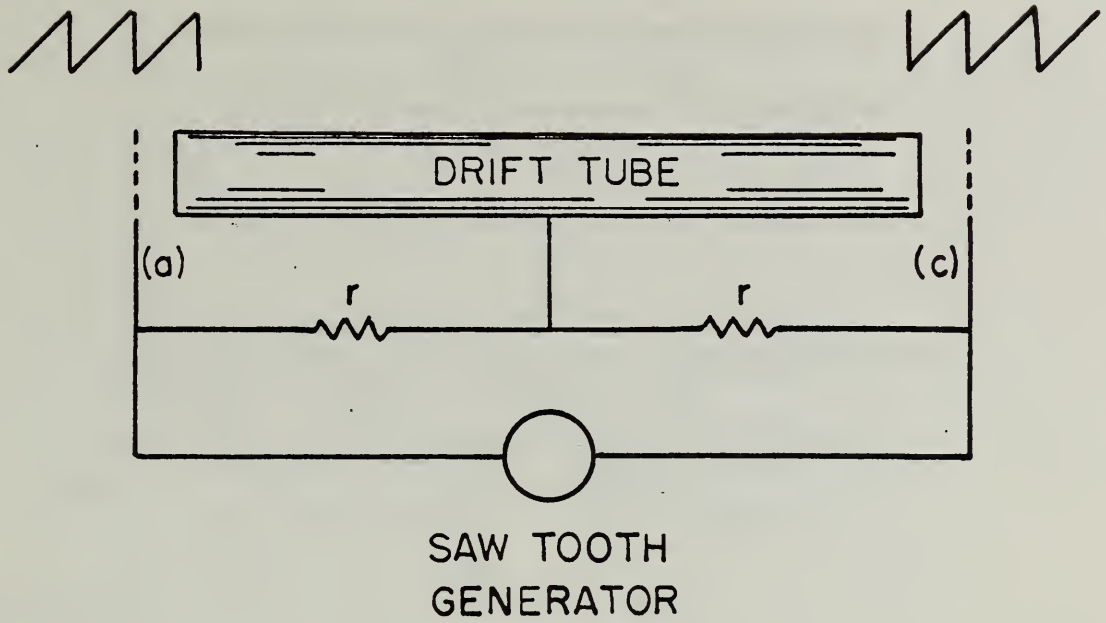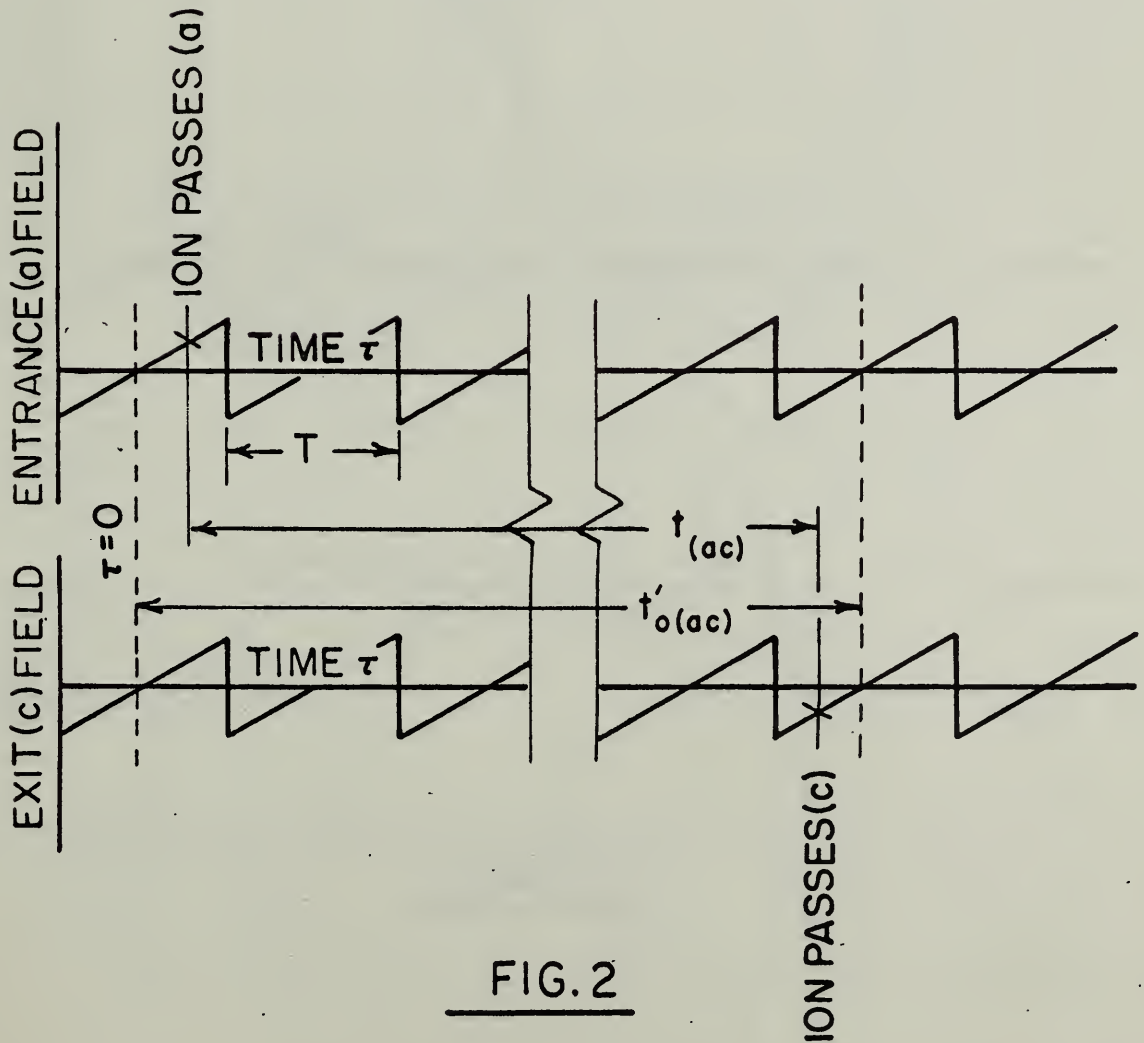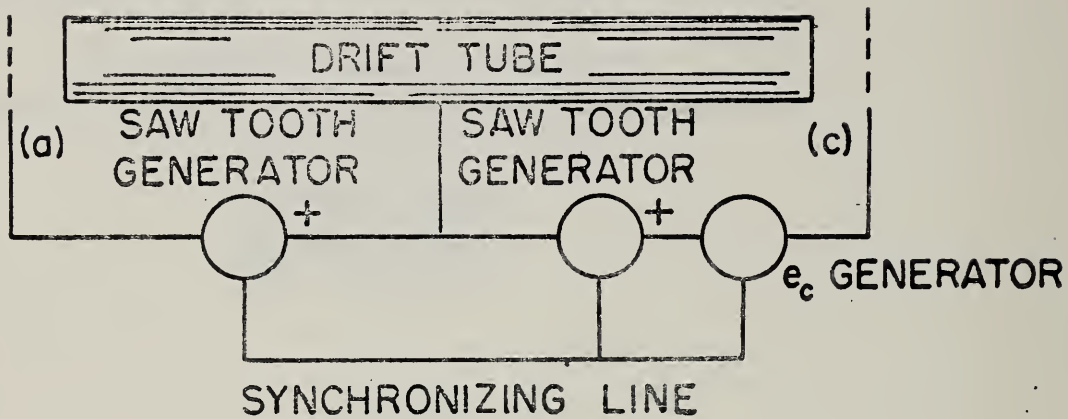
FIG. 3
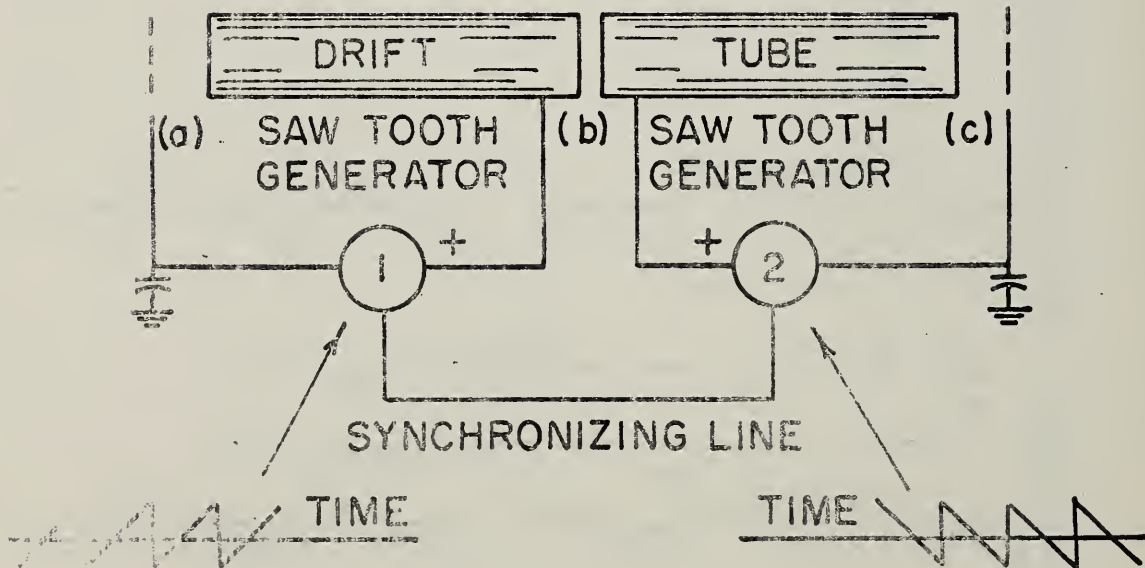
FIG. 4
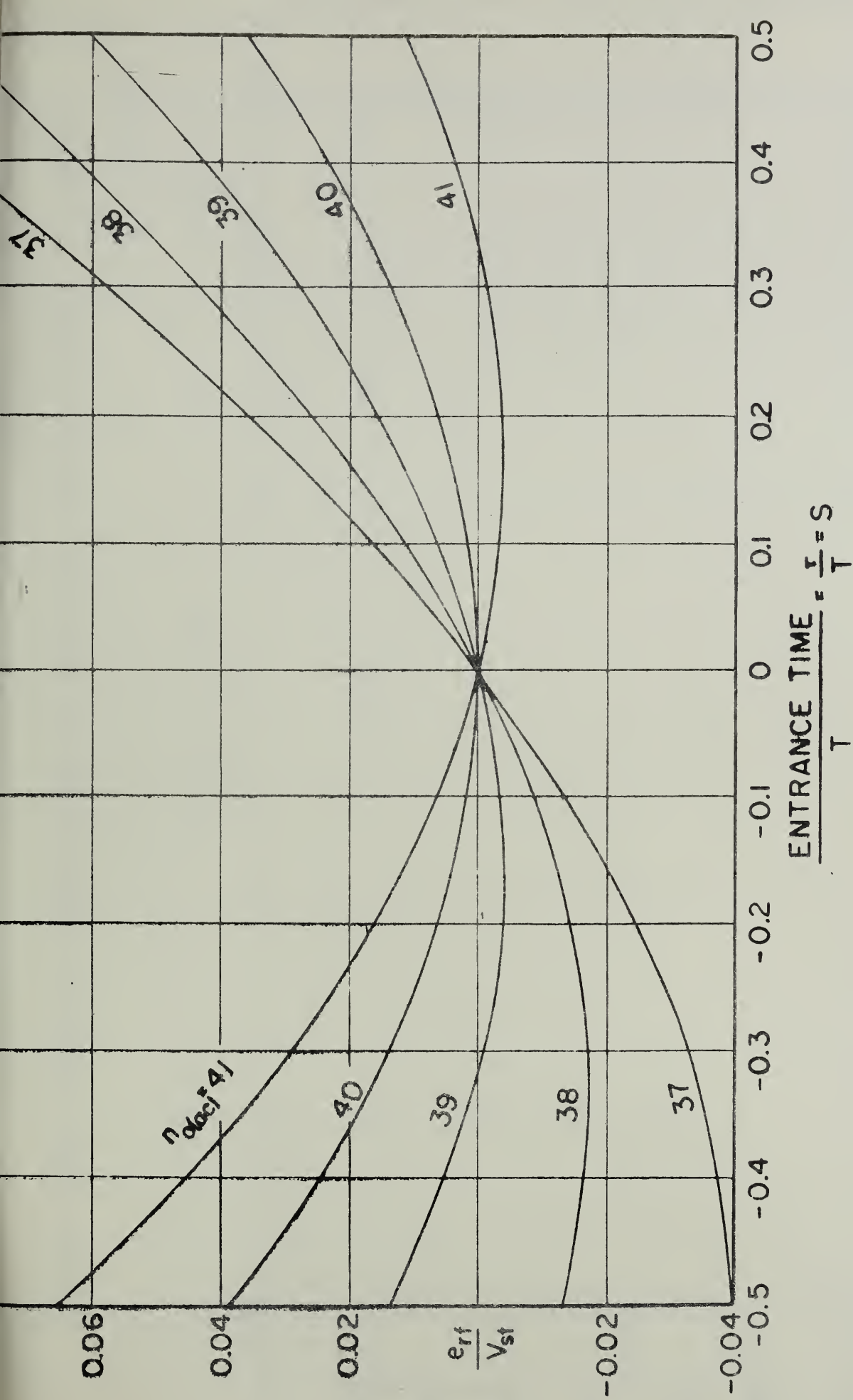
FIG. 5
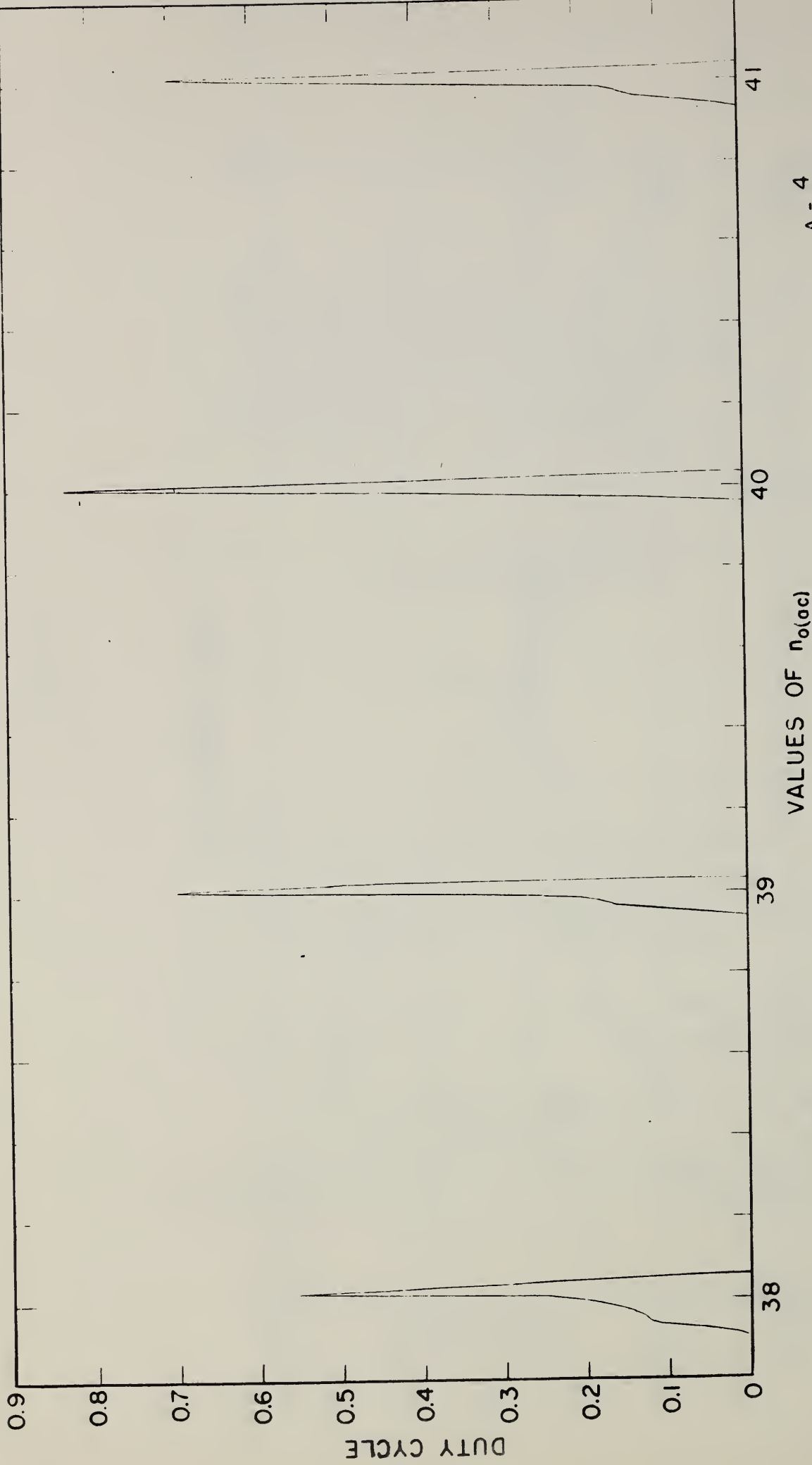
FIG. 6 - PEAK SHAPES USING SIMPLE VELOCITY MODULATION SCHEME

$A = \dfrac{4}{40}$

$0 < \dfrac{e_{rf}}{V_{st}} < 0.026$

VALUES OF $n_{o(ac)}$

DUTY CYCLE

FIG. 7

ENTRANCE TIME · S
                     T
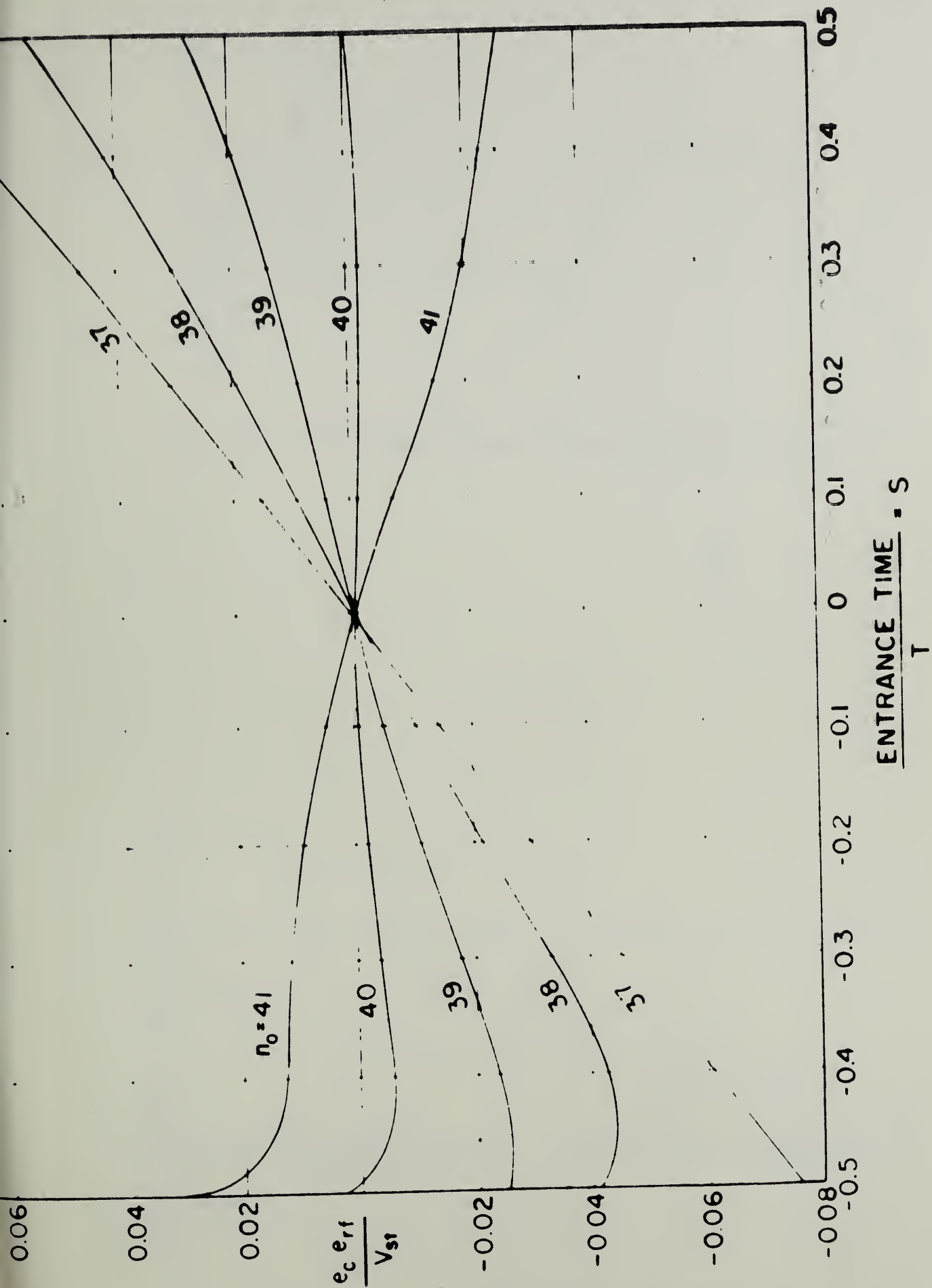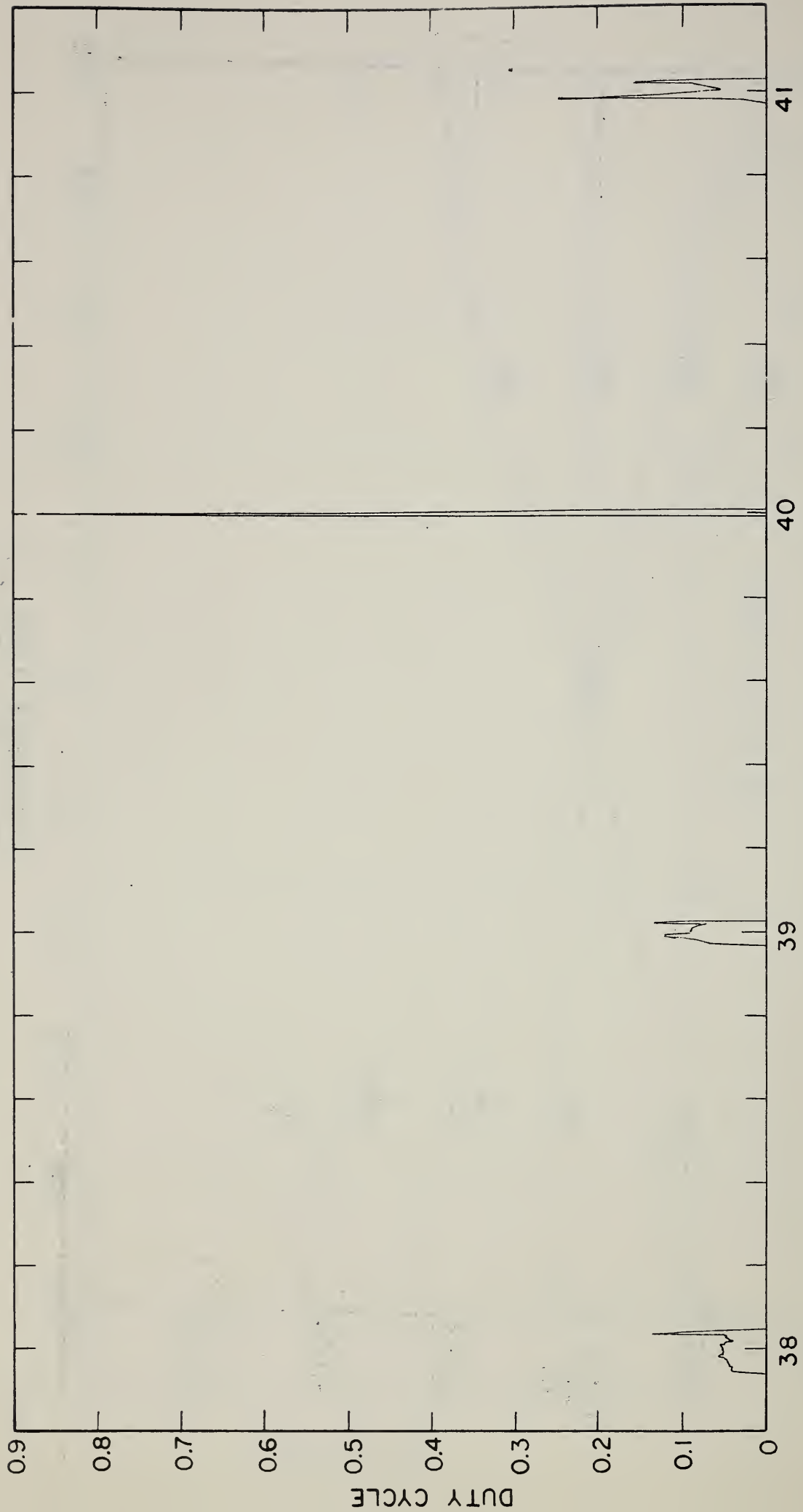
FIG. 8 — PEAK SHAPES USING CORRECTION WAVE
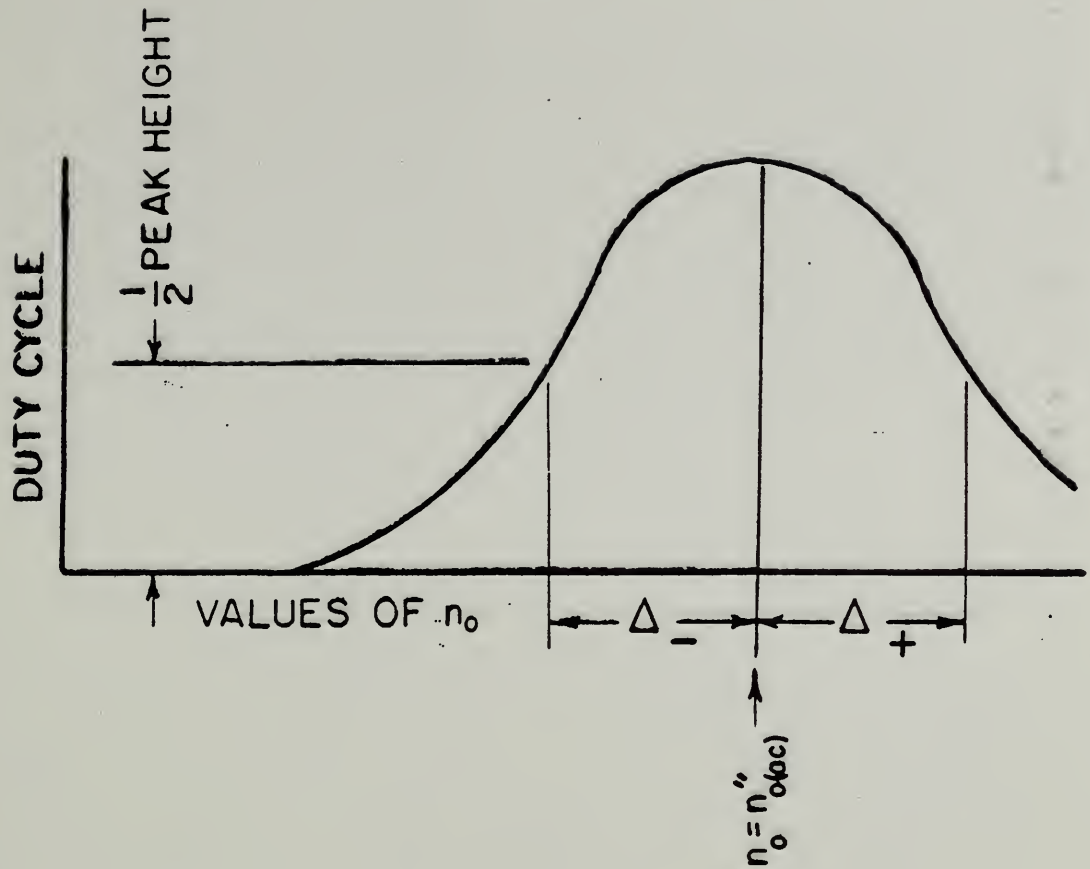
FIG. 9
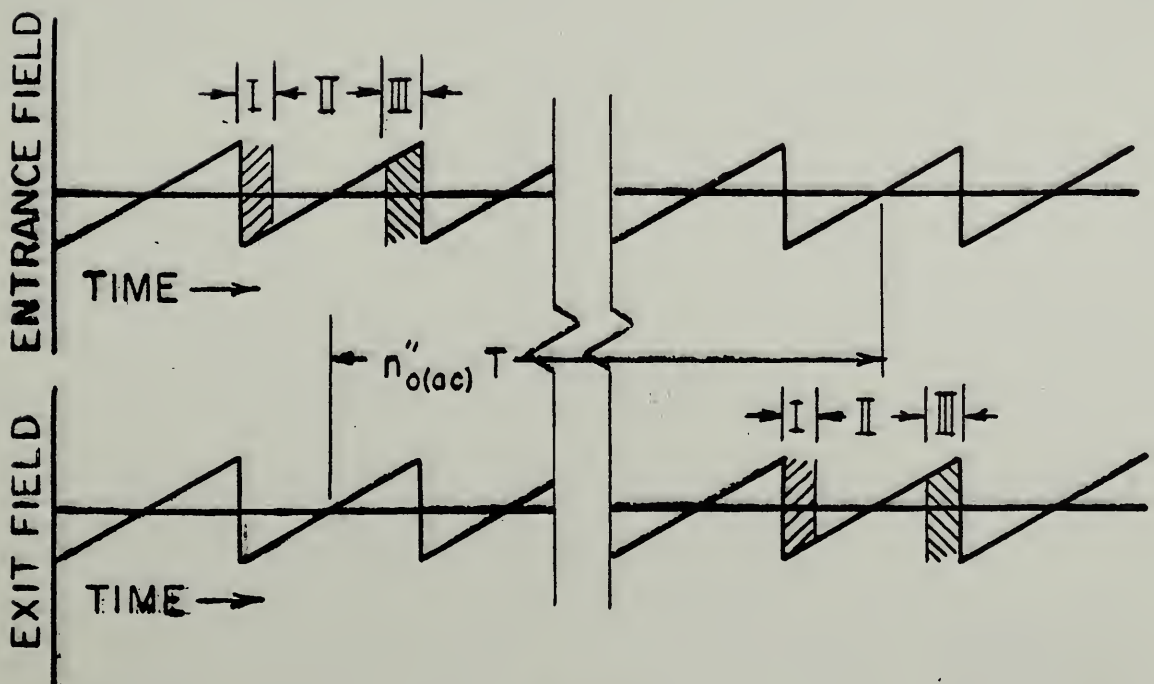
FIG. 11

$$\frac{V_{st}}{V_{dc}} \cong \frac{145}{3000}$$

ZERO SIGNAL

$n_{o(ac)} = 23.5$

$n_{o(ac)} = 26.5$
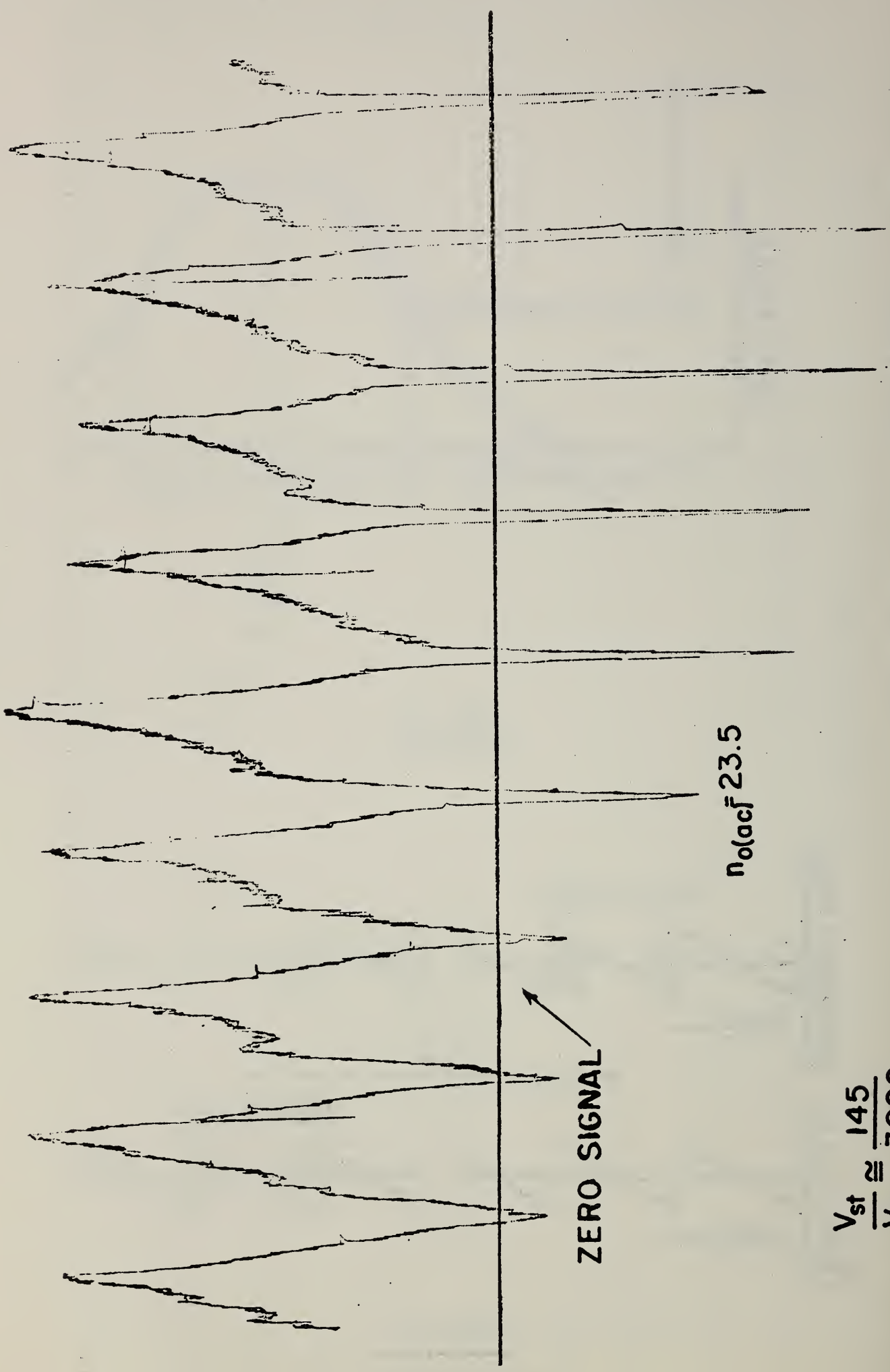
FIG. 10

THE NATIONAL BUREAU OF STANDARDS

The scope of activities of the National Bureau of Standards at its major laboratories in Washington, D.C., and Boulder, Colorado, is suggested in the following listing of the divisions and sections engaged in technical work. In general, each section carries out specialized research, development, and engineering in the field indicated by its title. A brief description of the activities, and of the resultant publications, appears on the inside of the front cover.

WASHINGTON, D. C.

Electricity. Resistance and Reactance. Electrochemistry. Electrical Instruments. Magnetic Measurements. Dielectrics. High Voltage. Absolute Electrical Measurements.

Metrology. Photometry and Colorimetry. Refractometry. Photographic Research. Length. Engineering Metrology. Mass and Volume.

Heat. Temperature Physics. Heat Measurements. Cryogenic Physics. Equation of State. Statistical Physics.

Radiation Physics. X-ray. Radioactivity. Radiation Theory. High Energy Radiation. Radiological Equipment. Nucleonic Instrumentation. Neutron Physics.

Analytical and Inorganic Chemistry. Pure Substances. Spectrochemistry. Solution Chemistry. Standard Reference Materials. Applied Analytical Research. Crystal Chemistry.

Mechanics. Sound. Pressure and Vacuum. Fluid Mechanics. Engineering Mechanics. Rheology. Combustion Controls.

Polymers. Macromolecules: Synthesis and Structure. Polymer Chemistry. Polymer Physics. Polymer Characterization. Polymer Evaluation and Testing. Applied Polymer Standards and Research. Dental Research.

Metallurgy. Engineering Metallurgy. Metal Reactions. Metal Physics. Electrolysis and Metal Deposition.

Inorganic Solids. Engineering Ceramics. Glass. Solid State Chemistry. Crystal Growth. Physical Properties. Crystallography.

Building Research. Structural Engineering. Fire Research. Mechanical Systems. Organic Building Materials. Codes and Safety Standards. Heat Transfer. Inorganic Building Materials. Metallic Building Materials.

Applied Mathematics. Numerical Analysis. Computation. Statistical Engineering. Mathematical Physics. Operations Research.

Data Processing Systems. Components and Techniques. Computer Technology. Measurements Automation. Engineering Applications. Systems Analysis.

Atomic Physics. Spectroscopy. Infrared Spectroscopy. Far Ultraviolet Physics. Solid State Physics. Electron Physics. Atomic Physics. Plasma Spectroscopy.

Instrumentation. Engineering Electronics. Electron Devices. Electronic Instrumentation. Mechanical Instruments. Basic Instrumentation.

Physical Chemistry. Thermochemistry. Surface Chemistry. Organic Chemistry. Molecular Spectroscopy. Elementary Processes. Mass Spectrometry. Photochemistry and Radiation Chemistry.

Office of Weights and Measures.

BOULDER, COLO.

CRYOGENIC ENGINEERING LABORATORY

Cryogenic Processes. Cryogenic Properties of Solids. Cryogenic Technical Services. Properties of Cryogenic Fluids.

CENTRAL RADIO PROPAGATION LABORATORY

Ionosphere Research and Propagation. Low Frequency and Very Low Frequency Research. Ionosphere Research. Prediction Services. Sun-Earth Relationships. Field Engineering. Radio Warning Services. Vertical Soundings Research.

Troposphere and Space Telecommunications. Data Reduction Instrumentation. Radio Noise. Tropospheric Measurements. Tropospheric Analysis. Spectrum Utilization Research. Radio-Meteorology. Lower Atmosphere Physics.

Radio Systems. Applied Electromagnetic Theory. High Frequency and Very High Frequency Research. Frequency Utilization. Modulation Research. Antenna Research. Radiodetermination.

Upper Atmosphere and Space Physics. Upper Atmosphere and Plasma Physics. High Latitude Ionosphere Physics. Ionosphere and Exosphere Scatter. Airglow and Aurora. Ionospheric Radio Astronomy.

RADIO STANDARDS LABORATORY

Radio Standards Physics. Frequency and Time Disseminations. Radio and Microwave Materials. Atomic Frequency and Time-Interval Standards. Radio Plasma. Microwave Physics.

Radio Standards Engineering. High Frequency Electrical Standards. High Frequency Calibration Services. High Frequency Impedance Standards. Microwave Calibration Services. Microwave Circuit Standards. Low Frequency Calibration Services.

Joint Institute for Laboratory Astrophysics-NBS Group (Univ. of Colo.).